

Elsevier required licence: © <2019>. This manuscript version is made available under the CC-BY-NC-ND 4.0 license <http://creativecommons.org/licenses/by-nc-nd/4.0/>

The definitive publisher version is available online at

[\[https://www.sciencedirect.com/science/article/abs/pii/S0893608019302175?via%3Dihub \]](https://www.sciencedirect.com/science/article/abs/pii/S0893608019302175?via%3Dihub)

Personalised Modelling with Spiking Neural Networks Integrating Temporal and Static Information

Maryam Doborjeh^{1,2}, Nikola Kasabov¹, Zohreh Doborjeh¹, Reza Enayatollahi³, Enmei Tu⁴, Amir
H. Gandomi^{5,6}

¹ Knowledge Engineering and Discovery Research Institute, Auckland University of Technology, Auckland, New Zealand.

² Computer Science Department, Auckland University of Technology, New Zealand.

³ BioDesign Lab, School of Engineering, Computer & Mathematical Sciences, Auckland University of Technology, Auckland, New Zealand.

⁴ School of Electronic Information & Electrical Engineering, Shanghai Jiao Tong University, China.

⁵ Faculty of Engineering and Information Technology, University of technology, Sydney, Australia

⁶ School of Business, Stevens Institute of Technology, Hoboken, New Jersey, USA

Abstract— This paper proposes a new personalised prognostic/diagnostic system that supports classification, prediction and pattern recognition when both static and dynamic/spatiotemporal features are presented in a dataset. The system is based on a proposed clustering method (named d2WKNN) for optimal selection of neighbouring samples to an individual with respect to the integration of both static (vector-based) and temporal individual data. The most relevant samples to an individual are selected to train a Personalised Spiking Neural Network (PSNN) that learns from sets of streaming data to capture the space and time association patterns. The generated time-dependant patterns resulted in a higher accuracy of classification/prediction (80% to 93%) when compared with global modelling and conventional methods. In addition, the PSNN models can support interpretability by creating personalised profiling of an individual. This contributes to a better understanding of the interactions between features. Therefore, an end-user can comprehend what interactions in the model have led to a certain decision (outcome). The proposed PSNN model is an analytical tool, applicable to several real-

life health applications, where different data domains describe a person's health condition. The system was applied to two case studies: (1) classification of spatiotemporal neuroimaging data for the investigation of individual response to treatment and (2) prediction of risk of stroke with respect to temporal environmental data. For both datasets, besides the temporal data, static health data were also available. The hyper-parameters of the proposed system, including the PSNN models and the d2WKNN clustering parameters, are optimised for each individual.

Keywords— *Integrated data domains, prediction, classification, personalised modelling, spiking neural networks, pattern recognition, environmental conditions, EEG data, Stroke.*

1. Introduction

An individual patient may have specific clinical, psychological, or behavioural factors which differ from other patients in the same category of diagnosis. These define the personal characteristics of each person that need to be considered for the tailoring of medical decisions, treatments, and practices toward precision medicine [1]. To this aim, scientists have recently suggested personalised treatments to sidestep undesirable influences of conventional treatments on the patient's current medical conditions (e.g., diabetes, heart disease, mellitus, and so forth).

In health and wellbeing studies, several researchers have contributed to improving decision making for a medical diagnosis for an individual. Literature has shown that personalisation is an effective technique to improve the performance of classification/prediction of previously unseen samples as reported in [2], [3]. In [4] a spiking neural network (SNN) architecture NeuCube for modelling brain data was proposed with the potential to be used for personalised modelling. Research [5] reported 83% accuracy of classifying patients with mild cognitive impairment (MCI) and those MCI patients with Alzheimer's disease (AD) using Magnetic Resonance Imaging (MRI) scans with respect to brain-age-related changes of an individual patient. In research [6], Quantum Associative Memories (QAM) was used for the diagnosis of tropical diseases (malaria symptoms versus different types of fevers) to improve the personal diagnostic process. Research [7] has developed a mechanical-left-ventricle model (MV) to build computational cardiac

modelling of 27 healthy controls and 11 patients with post-myocardial infarction (MI). The results suggested that myofibril active tension is greater in patients with MI than healthy individuals. This research was further developed towards personalised determining patients' sudden cardiac death after an acute MI [8].

The above computational modelling approaches performed successfully in a specific domain of data to build a personalised model for an individual. However, construction of a precise model for a person can be a challenging task when a massive amount of static vector-based, temporal or spatiotemporal (dynamic) datasets are available across many individuals.

Different multidimensional data domains are surrounding an individual and their interactions severely affect the personal risk and outcome. Understanding of these multimodal interactions requires an integration of several data sources to discover the “unknown” informative association patterns. Numerous personal events for an individual patient can be accurately classified/predicted if different sources of information can be integrated into a resultant unifying computational model that learns the complex patterns “hidden deep” in multivariate data.

Besides the accuracy of the decision making in machine learning, the model interpretability is also a crucial of importance in wellbeing study. This refers to understanding the relationships between the model's features and the predicted outputs, which has not been investigated in depth. The higher the interpretability of a model, the easier it is for an end-user to comprehend why certain decisions (output predictions) were made. This allows for knowledge discovery in the models and contributes to understand what interactions in the model have caused an event to occur. Nevertheless, the existing analytical methods often develop models on data without investigating the model learning patterns itself. Hence, they act as a “black-box” information processing system that solve a problem without discovering the causal relationships that have triggered the output. In personalised modelling method and system were proposed that include an integrated optimisation of personalised features, a cluster of neighbouring data from a database and the parameters of

a classification/prediction model. The proposed system uses vector-based, static personalised data. In [9] this approach was extended with the use of a spiking neural network (SNN) NeuCube [4] to model personalised spatiotemporal data after the static data are used to capture the cluster of neighbouring data.

The selection of a cluster of neighbouring data and parameter optimisation of a personalised SNN model are crucial for obtaining optimal personalised output results. To address these challenges and inspired by the importance of improved personalised treatment, this paper proposes a new personalised modelling approach that aims to develop a computational prognostic and diagnostic system that can integrate, in a novel way, both static and temporal/spatiotemporal data to improve decision making for an individual. This is based on the proposed here new integrated clustering method for the selection of neighbouring individuals to a person x using integrated static and temporal data for the individual. Then, selected temporal data are used as the training set for building an optimised SNN personalised model of this person.

Using SNN that represent information as action potentials (spikes) at a given time, offers some advantages when dealing with temporal data [9, 10, 11, 12]. An action potential occurs when the membrane potential of a specific axon location rapidly rises or falls in precise timing, called spikes¹. A sequence of spikes represents the times in which a neuron emitted action potentials.

Some of the SNN's characteristic features are: combined representation of temporal and spatial components of data; fast data learning as data is represented by binary events (spikes); time-based and frequency-based information representation. For these reasons, SNN can be considered as suitable techniques for spatiotemporal/temporal data modelling and analysis. Thus far, SNNs have been used for extracting patterns in different types of spatiotemporal data, such as functional MRI [10] and Electroencephalogram (EEG) [11].

¹ Spike is a binary value (-1 or 1) at time t , which represents a certain upward or downward change in the signal.

In this paper, the proposed personalised modelling system is based on a new clustering method and SNN architecture that contributes to the recognising of vital individual features, to the creation of personalised profiling, and the improvement of classification/prediction accuracy of output as compared to global modelling and conventional classifiers.

The proposed approach allows to:

- Select the most relevant neighbouring data to a new person's data.
- Build an optimised personalised model based on integrated static and dynamic data using contemporary neural network techniques –SNN that can incorporate both space and time information into one unifying model.
- Improve the model interpretability to perform as a decision support system.
- Evaluate how a personalised model can enhance the accuracy of outcome classification/prediction for a person.

The feasibility analysis of the proposed personalised modelling system is validated using two case study applications (Section 3.1 and 3.2).

2. A Predictive Personalised SNN Architecture for Learning Static and Temporal/Spatiotemporal (Dynamic) Data

In contrast to the global modelling, which uses all the samples in a dataset to build a model for a person x , the proposed personalised modelling system uses only a subset of samples which belongs to the relevant individuals to person x . The subset of samples is selected with respect to a new clustering method for integrated static and dynamic data. This subset data is utilised for the training process in an SNN model. SNN models have shown their potential to achieve incredibly high power efficiency as presented in several studies, such as pattern classification [12], [13], object recognition [14] and information encoding [15].

Therefore, we use here SNN because of their ability to learn changes in temporal data, represented as spikes and the interaction between these changes across many variables [9].

Our proposed personalised modelling system is designed according to the following phases:

1. Clustering of static and dynamic data by means of a new algorithm, named d2WKNN (dynamic Double Weighted-Distance K-Nearest Neighbours). For a new individual sample x , represented by both static and dynamic data, the involvement of each of the k neighbouring samples is ranked according to their integrated static and dynamic distances to x , giving higher ranks to the closer neighbours. This method results in extracting the relevant subset of samples for personalised modelling.
2. The selected samples are utilised to develop a Personalised Spiking Neural Network (PSNN) model.
3. The PSNN model is used to create an analytical profile for an individual and to achieve the best possible accuracy of prediction/classification of outputs for this individual. The personalised profile also enhances the interpretability of the model.

In the following sections, the above steps are explained in detail.

2.1. The Proposed Dynamic Double Weighted-Distance K-Nearest Neighbour Clustering Method

For a new person x , for whom both static and dynamic (temporal or spatiotemporal) data are available, an integrated static and dynamic data clustering procedure is accomplished through the following three parts:

- A. Forming a cluster (denoted by C_S) in a static data space $S^{N \times V}$, as nearest neighbouring samples to the sample x . There are N vector-based samples and V variables.
- B. Forming a cluster (denoted by C_T) in a spatiotemporal/temporal data space $T^{t \times f}$, as nearest neighbouring temporal samples to the sample x . Each sample is presented by a 2-dimensional matrix, where t time points are on the rows, and f variables are on the columns.

C. In order to take into account the relationship between temporal samples in cluster C_T , the selected temporal samples are subsampled again to obtain the most relevant samples to x . The subsampling procedure is explained later in this paper.

At step A, standardisation was used to transfer the static data, which might be recorded from different sources, into a consistent format. In the proposed d2WKNN method, the first W is defined by the normalised Euclidean distance between a sample vector x and other samples in the static data space. In the WWKNN method, which was earlier proposed in [9], one more ranking (weight) was introduced to include the variables' importance in the computation. When calculating the Euclidean distance in a V -dimensional space of input variables, it is typically supposed that all variables enumerate the same influence on the output. However, variables can be ranked by their discriminative power across samples belonging to different classes. This ranking can be used as the second weight (W) in our proposed method. This is computed here using the Signal-to-Noise Ratio (SNR) [16] which assesses how important a variable is to separate samples from different classes, one class named as 'signal' and the rest as 'noise'. In a C -class problem, where $C = \{1, 2, \dots, n\}$, for each variable v the SNR is defined as follows:

$$R_v = \frac{\sum_{i=1}^n \frac{\text{abs}(\mu_{i_v} - \mu_{\{C \setminus i\}_v})}{\sigma_{i_v} + \sigma_{\{C \setminus i\}_v}}}{n}, v = 1, \dots, V \quad (1)$$

where i shows which class is named as a signal, while $\{C \setminus i\}$ is a set difference in 'set theory' which represents the rest of the classes as noise. Therefore, σ_{i_v} and μ_{i_v} are correspondingly the standard deviation and the mean value of the variable v among all the samples in class i . Then R_v vector is used to weigh the normalised Euclidean distance $D_{x,y}$ between a sample vector x and another sample vector y as follows:

$$D_{x,y} = \frac{\sqrt{\sum_{v=1}^V R_v (x_v - y_v)^2}}{\sum R_v} \quad (2)$$

For a new sample x , we selected a subset of k samples to form a cluster C_s , so that each computed distance to x ($D_{x,y}$, where $y = \{1, \dots, N - 1\}$, $N =$ number of samples) is less than an adaptive distance

threshold α . The threshold α is initially set to the mean value of the distance ($\mu D_{x,y}$) and then modified through optimisation. The distance $D_{x,y}$ in relation (2) is computed based on the static data. However, as the dataset contains both static and temporal data, a new distance needs to be computed in respect to the temporal data space.

At step B, we considered only those temporal data samples (named cluster C_T) that belong to the individuals in the cluster C_S . The class information is also assigned to each sample in C_T . In order to compute the distance between these temporal samples, a time-alignment distance measurement, called Dynamic Time Warping (*DTW*) [17], is used. In contrast to the Euclidean distance, which computes a point-to-point distance, the *DTW* method allows for many-to-one point comparisons to find a global optimal alignment between time series. The *DTW* method allows to compute an optimal match between the two time-series as follows:

For time series $A = \{a_1, \dots, a_n\}$ and $B = \{b_1, \dots, b_m\}$ with lengths of n and m correspondingly, an alignment by $DTW(A, B)$ represents a time-warping matrix $M^{n \times m}$ which contains the distances between the i^{th} point of A to the j^{th} point of B , where $1 < i < n$ and $1 < j < m$, as shown in Fig. 1.

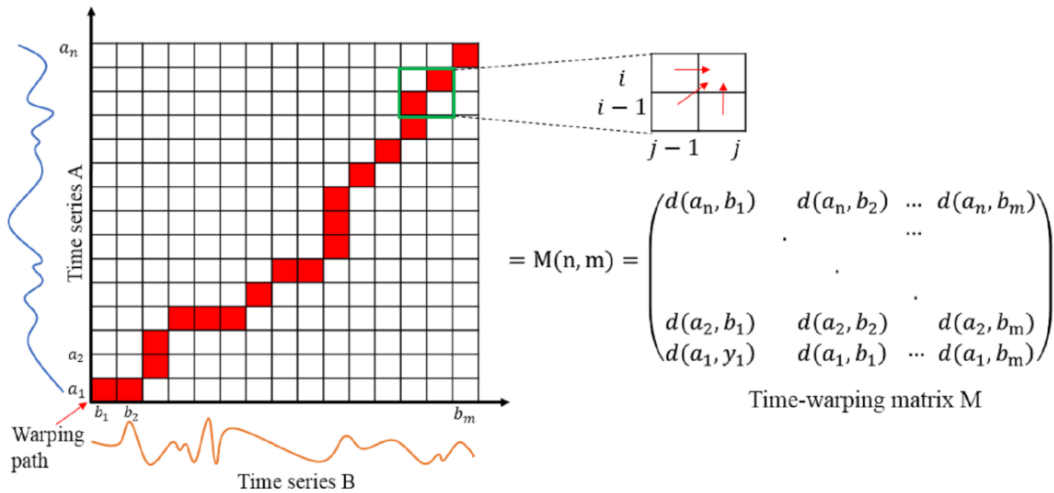


Fig. 1. A time-warping matrix that illustrates an optimal similarity path (shown in red) between the two time-series A and B.

Each distance $d(a_i, b_j)$ in the matrix M is computed as follows:

$$M(i, j) = d(a_i, b_j) = \|a_i - b_j\| + \min \begin{cases} \|a_i - b_{j-1}\| \\ \|a_{i-1} - b_j\| \\ \|a_{i-1} - b_{j-1}\| \end{cases} \quad (3)$$

where $\|a_i - b_j\|$ denotes to $(a_i - b_j)^2$ as shown in the cell (i, j) of the warping matrix M . The objective in $DTW(A, B)$ is to obtain the optimal path $W = \{w_1, \dots, w_k\}$ in the M matrix through minimising the function below which identifies the shortest path in W :

$$DTW(A, B) = \left(\sum_{k=1}^K w_k \right); \quad k = \text{length of the path } W \quad (4)$$

The $DTW(A, B)$ distance shows the degree to which the two time-series A and B are similar. Using the DTW distance, we can rank the temporal samples with respect to their time-dependent distance to the new sample x , where the higher the rank indicates the greater the distance between the time series. Once the DTW distances between the temporal samples are computed, the C_T will be subsampled using the Silhouette coefficient [18] which validates the homogeneity within a class of samples by measuring how similar a sample is to its own class (cohesion) compared to other classes (separation). This is performed as follows:

1. Class label information is assigned to the temporal samples in cluster C_T .
2. The Silhouette value is computed for each sample as follows:

For each sample i which belongs to a class c , the $x(i)$ is the average cohesion of i to all other samples in the same class as follows:

$$x(i) = \sum_{j=1}^n DTW(j, i) \quad (5)$$

$DTW(j, i)$ computes the distance between temporal sample i to other n temporal samples in the same class. It shows how well sample i fits into its own class so that a smaller distance value refers to a better

assignment. In contrast, $y(i)$ denotes to the separation between sample i from the current class and samples in another class. The Silhouette value for sample i is presented here as follows:

$$s(i) = \begin{cases} 1 - \frac{y(i)}{x(i)}, & \text{if } x(i) > y(i) \\ 0, & \text{if } x(i) = y(i) \\ \frac{x(i)}{y(i)} - 1, & \text{if } x(i) < y(i) \end{cases} \quad (6)$$

The silhouette value is in the range of $-1 \leq s(i) \leq 1$, where a value closer to 1 represents that the sample is well matched to its own class.

At that point in order to subsample the C_T cluster, in each class we extract samples with high Silhouette values (larger than an adaptive threshold s_θ that can be modified by optimisation). Through this, several samples are selected. Then the Silhouette distance between the selected samples and the rest of the samples are measured. After that, every selected sample forms a cluster of samples around itself if the absolute values of Silhouette distances between them are less than a radius $\beta = 0.4$. Finally, a cluster with greatest number of samples is selected as it has the highest density. The density is defined with respect to the number of samples within the radius β . This set of samples are considered as the most relevant neighbouring samples to person x , extracted with respect to both static and dynamic data. A block diagram of the proposed personalised modelling framework is presented in Fig. 2.

Fig. 2(a) shows that for an individual i , a cluster of samples with similar static data to i is selected. Then with respect to these selected samples, relevant temporal samples are extracted, as shown in Fig. 2(b). It can be seen from Fig. 2(b1) that the selected temporal samples may have an overlapping distribution across different classes (in this example a two-class problem A and B). In order to select the most relevant temporal samples, we computed a silhouette value for each sample, by measuring the separation and cohesion as shown in Fig. 2(b2-b4). As a final point, Fig. 2(b4) illustrates the sub-clusters of samples which have high silhouette values (greater than a silhouette threshold) and have the largest number of neighbouring samples (when a cohesion threshold is applied). These samples are then passed into a 3-dimensional PSNN model

for unsupervised learning. The trained model will be tested for prediction/classification using the temporal samples of individual i , which were excluded from training. For an individual, the selected group of samples (number of training samples) can be different with respect to the parameter setting in the proposed d2WKNN algorithm. If we set the parameters to the optimised values, then the same samples will be selected for training anytime we run the experiment. This aims at achieving stability.

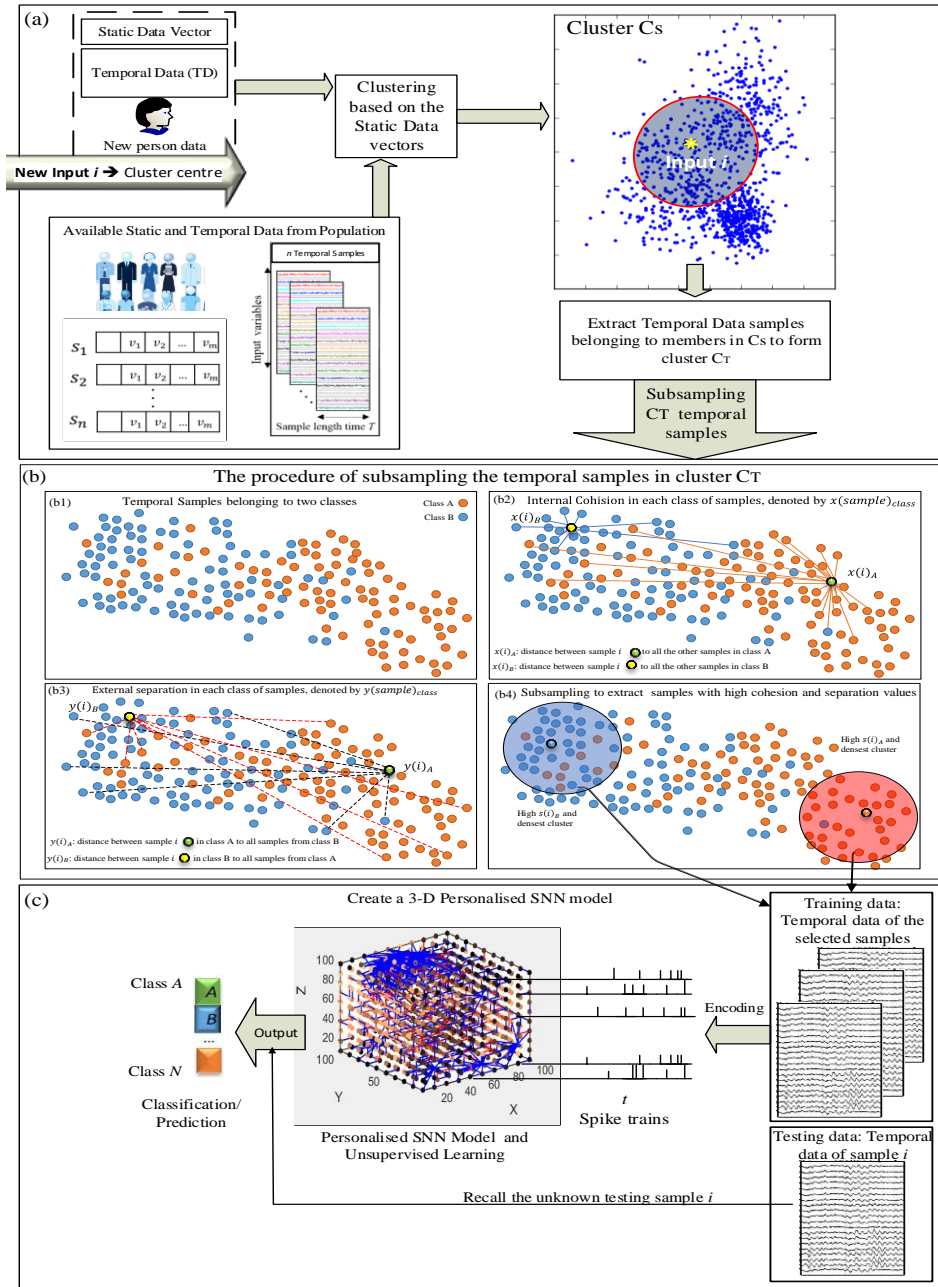


Fig. 2. The general schema of the proposed personalised modelling system for learning and modelling of integrated static and temporal data. (a) For individual i , a cluster of samples with similar static information to i is selected; (b1) An example of overlapping clusters of samples' distribution in two-class problem— A and B; (b2) An example of computing the cohesion values between one selected sample and other samples; (b3) An example of computing the separation values between one selected sample from class A to all the samples in class B (and the opposite way as well); (b4) The high-density sub-clusters of samples are selected; (c) The final selected temporal samples are passed into a 3-dimensional PSNN model to map the spatial information and learn the temporal patterns. The trained model will be tested for prediction/classification using the unseen temporal samples of individual i (were excluded from training).

2.2. Predictive Personalised Spiking Neural Network (PSNN) Model

The selected nearest neighbouring samples to an individual i are used to build a PSNN model through the following steps using the NeuCube SNN architecture [5]:

1. Encoding the input spatiotemporal/temporal samples into spike trains, which encodes certain changes in the data over time.
2. Create a recurrent PSNN architecture for spatial mapping of the variables. This preserves the spatial relationship between data variables.
3. Deep-in-time unsupervised learning in the PSNN model to capture the spatiotemporal relationships between variables while streaming the input data.
4. Supervised learning in an output layer classifier to learn the association between the input data and the class label information.
5. Recall the spatiotemporal/temporal samples of individual i (were excluded from training) to cross-validate the model for classification or early prediction of outcomes. For the prediction task, a smaller length of the testing data is used to identify how early the best prediction can be achieved. For the classification task, the whole length of the testing data is used.
6. The above steps are embedded in an optimisation process.

The organisation of the training and testing data is shown in Fig. 3. When the SNN model is trained with related samples to an individual i , then the model will be tested using samples from individual i which were excluded from the training phase. This is like leave-one-out cross-validation, but instead of training the model with $N - 1$ samples (N is the number of samples), we train the model using the most related samples to x .

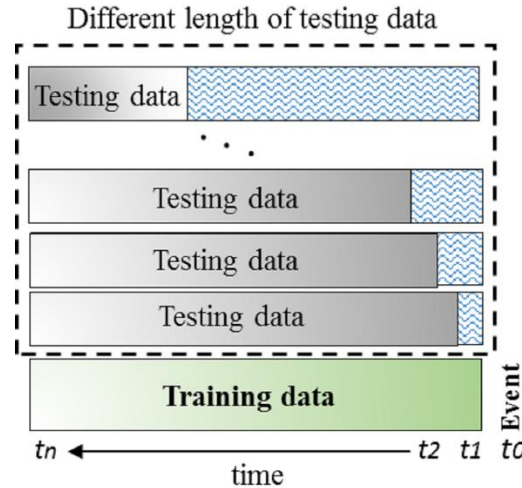


Fig. 3. The scheme of the selection of training and testing datasets for early prediction of an event. The green bar represents the time-window for training samples with a length of t_n , while the grey bars represent the different lengths of the testing sample that start from t_n and step down until the best early prognostication time point is detected.

2.2.1. Computational Model of Spiking Neuron in a PSNN

In a biological neuron structure, when the overall power of input signals goes beyond a threshold, an action-potential is produced and sent to other neurons connected to it. Therefore, neurons receive, process and transmit input information by means of electrical signals exchanged via synapses. Artificial spiking neurons can computationally simulate this procedure as information-processing units that accomplish non-linear processing [19], [20], [21], [22], [23]. A collection of interconnected spiking neurons creates an SNN, where their spiking activities influence neighbouring neurons. Resembling a biological neuron, in SNN architecture, incoming spikes make changes in a neuron's potential, and once this surpasses the neuron potential (a threshold value), the neuron emits an output spike. Similar to the axons, artificial neurons are interconnected through simulated paths, which are initially established with random weights. Then the neuron's synaptic strengths are adapted through spike communications across synapses. Fig. 4 illustrates a biological neuron and a simulated artificial spiking neuron which resembles the behaviour of a biological neuron's cell.

When an SNN is used for learning temporal data, such data first needs to be encoded into sequences of spikes which are then transferred into the SNN via input neurons. Throughout the learning procedure, the

synaptic weights in the SNN are adjusted with respect to continues incoming spikes, which are incrementally processed at each neuron.

2.2.2. Input Data Encoding.

Spike-time encoding is inspired by the neural encoding processes in neurobiology that transfer neural signals into electrical pulses, so-called spikes or action potentials. Different spike encoding algorithms have been proposed, some popular ones are: temporal encoding [24], [25], [26], [27], Ben's Spikes Algorithm (BSA) [28] and Population Rank Coding [29].

For the encoding procedure here, a threshold-based encoding technique is used to produce excitatory (positive) and inhibitory (negative) spikes, so that the dynamics of the data are preserved. In our paper, for a signal of length $T = \{t_1, \dots, t_n\}$, if the upward change in the signal exceeds an encoding threshold β at time t , then a positive spike is generated and positioned at the corresponding time point t . In contrast, if the downward changes surpass the β value, then negative spikes are generated.

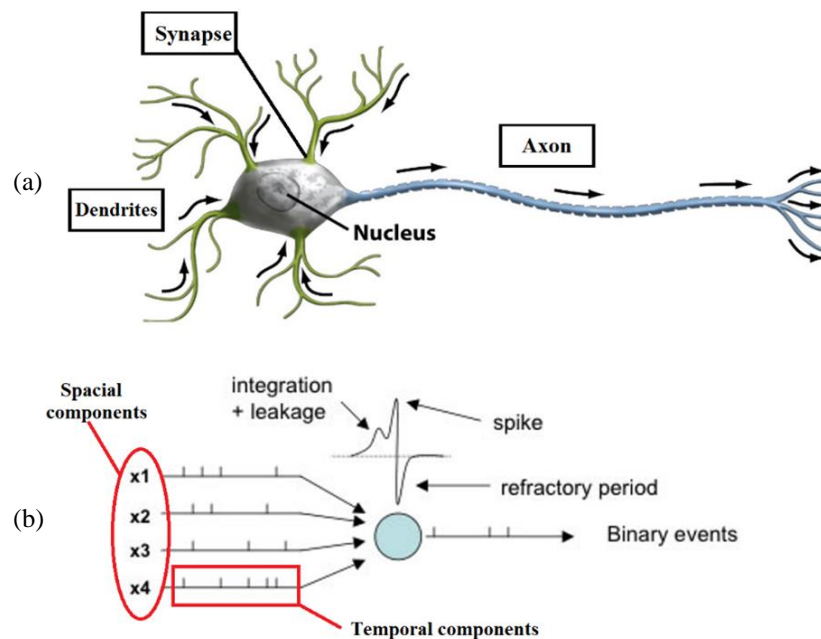


Fig. 4 (a) Structure of a biological neuron which receives input information across axon terminals, (modified from [30]); (b) Artificial spiking neuron which receives input spike trains, processes them and produces output spikes with respect to the leaky integrate-and-fire model of a neuron [31].

2.2.3. *Spatial Mapping of Input Variables into a PSNN Model*

A PSNN model has a 3-Dimensional structure of a suitable size that preserves the spatial information of data if such information exists, or alternatively preserves it with respect to the temporal similarity between input temporal features. If the spatial information of temporal data variables is given, we can spatially map these variables into their exact 3D positions in a pre-designed PSNN model. For instance, in the case of spatiotemporal brain data such as EEG, the PSNN model spatially maps a brain template such as Talairach [32]. Then the EEG channels are positioned in the PSNN model as input neurons using the same coordinates as in the brain template. If such spatial information is not available for some datasets, then temporal variables can be efficiently mapped to a PSNN model with respect to their temporal correlation. For mapping of such input temporal variables to the PSNN model, we used a Graph Matching Optimization (GMO) algorithm [33] in which the highly correlated variables are assigned to topologically close input neurons in the PSNN model. The correlation is computed with respect to the encoded spike trains and a high positive correlation represents that the variables are well time dependent.

2.2.4. *Initialisation of a PSNN Model*

A PSNN model is initialised using the small-world (SW) connectivity [34], rule (as can be seen in [35] [4], [36]), that is inspired by biological systems [37], [38]. The SW generates random connections from a neuron n_i to nearby neurons within a neighbourhood radius. The connection $w_{i,j}$ from neuron n_i to n_j is initially weighted as follow:

$$w_{i,j} = \frac{r_{ij}}{d_{i,j}}; r \in \mathbb{R}_{[-1,1]} \quad (7)$$

where $d_{i,j}$ is the distance between two neurons n_i and n_j .

Spiking neurons in the PSNN can be implemented using different computation models such as Lapique [39], Integrated-and-Fire Model [40], [14], Izhikevich Model [41]. In this paper, we use Leaky integrate-and-fire model (LIFM) of a neuron [31]. Like a biological neuron, in LIFM when a neuron emits a spike, it

does not produce a new spike within a refractory period and its membrane potential $v(t)$ leaks by a parameter τ . The neuron action-potential is defined in relation (8), where τ_m denotes to the membrane time constant, v_{rest} defines the resting potential, and R and I are respectively the resistance and the input current.

$$\tau_m \frac{dv}{dt} = v_{rest} - v(t) + RI(t) \quad (8)$$

2.2.5. Deep-in-time Unsupervised Learning in a PSNN Model

When a PSNN model is spatially mapped and initialised, the connection weights need to be modified while it is learning from input spike trains which are streaming to the model over time. At this phase of the learning, the desired outputs (class labels) are not provided and the training process is performed with unlabelled input data patterns. Hitherto, several unsupervised learning algorithms have been developed in SNN models, the majority of them are constructed to adapt the synaptic weights according to temporal relation between pre- and postsynaptic² action potentials as similarly implemented in Hebbian learning [42], [43]. One of the most popular examples of Hebbian learning is Spike-Time Dependent Plasticity (STDP) learning rule, which depends on the relative timing of pre and postsynaptic action potentials [42]. The STDP learning rule is defined using the following relation (9).

$$F(\Delta t) = \begin{cases} A_+ \exp(\Delta t / \tau_+) & \text{if } \Delta t < 0 \\ -A_- \exp(-\Delta t / \tau_-) & \text{if } \Delta t \geq 0 \end{cases} \quad (9)$$

$F(\Delta t)$ represents the connection weight modification caused by a pair of pre to postsynaptic spikes, separated by a time interval Δt . The parameters A_+ and A_- refer to the maximum values for the synaptic modification, which transpire when $\Delta t \approx 0$. The parameters τ_+ and τ_- control refer to the ranges of pre-to-postsynaptic inter-spike intervals over which the synaptic strengthening and weakening occur. In the proposed PSNN model, the connections are adapted over time that represent patterns of connected clusters of neurons, similar to deep neural networks [44]. However, the adapted spatiotemporal connections here

² Presynaptic neuron is delivering the “message” across the synapse to the postsynaptic neuron. The postsynaptic neuron is the “receiver” of the neurotransmitter “message” from the presynaptic neuron.

are not being constant as a fixed structure (fixed number of neurons and layer) as Convolutional Neural Networks (CNN) [45]. It means that in SNNs, during the learning procedure different connections are modified differently with respect to the time that spike transformation occurs. In contrast to the typical multi-layer perceptron networks, neurons in the SNN do not fire at each propagation cycle. They fire only when their membrane potentials – as intrinsic quality of the neuron related to its membrane electrical charge – reach a specific value. In the trained SNN model, neurons that were not involved in the information transformation and the connections with weak values can be removed from the reservoir. Therefore, the SNN model will have as many neurons and connections as needed for processing a specific task. Therefore, STDP evolves the neuronal connection weights reflecting the dynamics of the brain data that relate directly to the brain process.

2.2.6. *Supervised Learning in a PSNN Model using Dynamic Evolving SNN*

During the unsupervised learning with temporal pattern of the input spike trains, connection weights are learnt in the PSNN model, that represent spatiotemporal interaction between temporal variables over time. Afterwards, a supervised learning is performed to learn the associations between the captured patterns in the PSNN model and the training samples' class label information. For this purpose, the same training samples are propagated to the trained PSNN model again, and the spiking activity of the PSNN model is utilised for the training of an output classifier. For each sample in the training dataset, one output neuron is created and fully connected to neurons in the already trained PSNN model. We used dynamic evolving SNN (deSNN [46]) for the output classifier. The connection weights from neurons in the PSNN model to an output neuron j are first set to zero and later initialised using Rank-Order rule (RO) [47] wherein the first incoming spike from a neuron i in the PSNN model to an output neuron j has the highest value of the corresponding connection $w_{i,j}$ as follow:

$$w_{i,j} = \sigma Mod^{order(i,j)} \quad (10)$$

where the learning parameter is denoted by σ , and Mod represents the modulation parameter which identifies the importance (rank) of the incoming spike with respect to the order in which a spike is entered to the output neuron ($order(i, j)$) among all the other arriving spikes. This allows the first spike to have the highest influence in increasing the value of W_{ij} . Then, W_{ij} will be further modified using a small parameter drift that considers the following spikes to neuron j at time t . While streaming the input training samples over time, the postsynaptic membrane potential ($PSP_j t$) of the output neurons j at time t increases until it surpasses a firing threshold as follows:

$$PSP_j t = \sum mod^{order(i)} W_{ij} \quad (11)$$

After the supervised learning is completed, at the recall phase, if a new spike train of an individual x enters to the trained PSNN model, a neuron i in the PSNN model emits an output spike if the $PSP_i t$ exceeds the firing threshold. This output spike is then transmitted to the output neurons positioned on the deSNN layer. This spike transmission modifies the corresponding connection weights $w_{i,j}$, where $j = \{1, \dots, number\ of\ training\ samples\}$, and the output neuron's $PSP_j t$ at the deSNN layer. When the $PSP_j t$ on the output layer exceeds the firing threshold, the neuron j produces an output spike at time t . To classify a testing sample x , a KNN method is used to vote to the class label of the top K output neurons from the classifier which fired earlier in time. In addition to detecting the class label ($c = \{1, \dots, C\}$) of the testing sample, the results can be interpreted as a probability p_x that shows how fit the sample x is to the detected class label compared to the other classes as follows:

$$p_x = \frac{\sum KNN_c}{K} \quad (12)$$

where $\sum KNN_c$ represents the number of voting to class c within the K neighbouring output neurons.

2.2.7. Parameter Optimisation of the PSNN

When building a PSNN model for an individual, the model is optimised using an exhaustive grid-search optimisation algorithm with an objective function of minimising the prediction/classification error through

optimal tuning of the model's parameters. We optimised two main parameters from the d2WKNN clustering procedure, and one hyper-parameter from the STDP learning procedure in the PSNN model as follows:

- Distance Threshold α in the clustering of static data: a radius parameter in which the nearest neighbouring samples are positioned.
- Silhouette threshold s_θ in the temporal data clustering: this identifies the temporal samples with small internal DTW distance to other samples in their own class while having large DTW distances to samples from other classes.
- Learning rate α : this is a parameter in the unsupervised STDP learning procedure in the PSNN model.

To obtain the best accuracy of classification/prediction, these three parameters α , s_θ , and α were optimised, so that for every individual the procedure of learning and testing was repeated 45 times as there were three values for α , three values for s_θ and five values for α as follows:

$$\begin{cases} \alpha \in [\mu D_{x,y} - \sigma D_{x,y}; \mu D_{x,y}; \mu D_{x,y} + \sigma D_{x,y}] \\ s_\theta \in [\mu s_\theta - \sigma s_\theta; \mu s_\theta; \mu s_\theta + \sigma s_\theta] \\ \alpha \in \left[l_{min}, \left(\frac{l_{max} - l_{min}}{stp} + (l_{min} \times i) \right), \dots, l_{max} \right] \\ i = 1, \dots, stp \end{cases} \quad (13)$$

where: y refers to each of the samples in the dataset (except x); $\mu D_{x,y}$ is the mean value of the normalised Euclidean distance between x and other samples; $\sigma D_{x,y}$ is the standard deviation of the distances; μs_θ is the mean value of the Silhouette values in a class; σs_θ is the standard deviation of the Silhouette values in a class; l_{min} and l_{max} are the minimum and maximum values for α ; and stp defines how many steps were chosen within the interval of $l_{max} - l_{min}$.

3. Case Studies of Personalised Modelling using the Proposed PSNN Model

The feasibility analysis of this approach is tested using two case study problems that represent the methodology as a generic one, applicable to different data domains. The first experiment is a classification of spatiotemporal EEG data across individuals belonging to different health categories (Sec. 3.1) to investigate the individual response to treatment. The second experiment relates to the early prediction of individual stroke occurrence in relation to temporal environmental data (Sec.3.2). For the case studies, both static vector-based and dynamic, temporal data are available per individual (Sec. 3.2).

3.1 Case Study 1: Classification Based on Static Clinical Data and Spatiotemporal EEG Data Related to Individual Response to Treatment

In this section, the proposed personalised modelling system is applied for determining individual response to a certain treatment with respect to integrated data sources. We used data [48], [49], [50] which were recorded under an ethical approval granted by the *Northern Regional X Ethics Committee of New Zealand*. The data were recorded at the School of Pharmacy, University of Auckland. All participants signed informed consent to certify their voluntary participation. The dataset contains both static and spatiotemporal data collected from each participant.

The spatiotemporal EEG data in this paper are from 67 participants (samples), in which 21 samples are categorised as a healthy control group (class 1—H), 29 samples are categorised as patients undertaking Methadone maintenance treatment (class 2—M), and 17 samples are labelled as opiate addict patients (class 3—P). The EEG signals were measured using 26 channels based on the “10-20” International System while participants were performing a psychological test which involved several brain functions and areas. Throughout the test, the word ‘PRESS’ was frequently shown (every 500 ms) on the screen in either green or red colours. Before the test began, participants were trained to react to the world appearing in green by pressing a button and not reacting to the ‘PRESS’ that presented in red. This kind of cognitive test is usually used to measure an individual’s ability for response control and sustained attention.

Along with the spatiotemporal EEG data, static vector-based data were also measured for each individual such as age, gender and drug consumption. In total, there were 20 variables for measuring the static information from each subject. Fig. 5(a) presents only 15 vectors of static data, randomly selected from these 67 individuals. The SNR values for these 20 variables of static data (67 instances) are computed and reported in Fig. 5(b). It represents that variable 2 (gender) has the highest importance in static data for discriminating the individuals into different health categories: healthy (H), under-treatment (M), and patient (P).

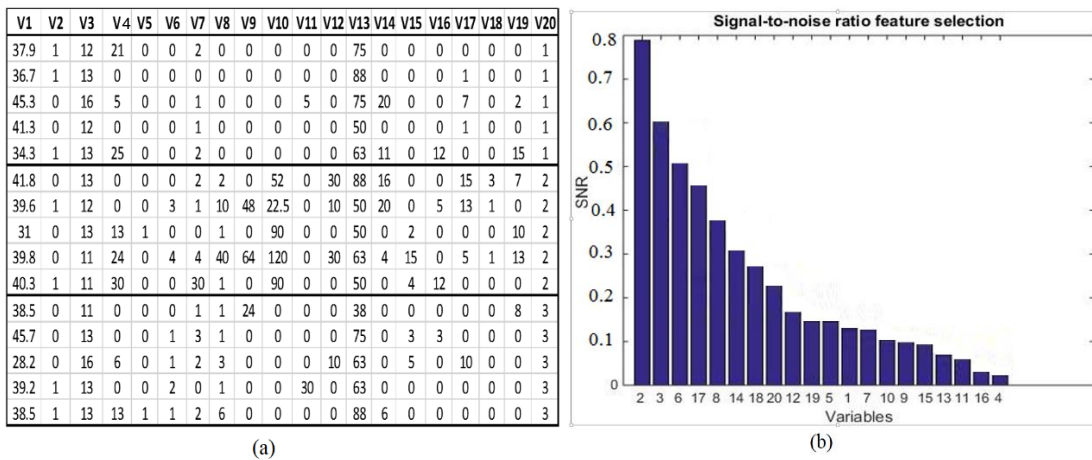


Fig. 5 (a) Five static data instances are randomly selected from each group of subjects (in total 15 instances are shown here). The static variables are V1: age; V2: gender (0 is male and 1 is female); V3: level of education; V4: life-time nicotine consumption; V5: illness; V6: history of overdose; V7: times of hospitalised; V8: Legal charge; V9: days being in jail; V10: Methadone dose; V11: alcohol consumption in last 30 days; V12: sedative consumption in last 30 days; V13: level of anger; V14: cannabis consumption; V15: hallucinogens consumption; V16: taking ecstasy; V17: amphetamine consumption; V18: barbiturate consumption; V19: heroin; and V20: level of fear. Class labels of subject groups are: 1 is healthy, 2 is treatment, and 3 is patient. (b) The SNR values for the variables in static data.

Fig. 6 illustrates the in-house developed user-interface of the personalised modelling system to classify individual health outcome with respect to the integrated static clinical data (from Fig. 5) and the spatiotemporal EEG data. The number of the selected nearest samples for each individual here (K) is not only varied person to person, but also varied for a particular person respecting different model's parameters such as distance threshold α and Silhouette threshold s_θ , which are correspondingly the neighbourhood radius in the static and spatiotemporal data spaces.

When the EEG data of the most relevant samples to an individual are extracted, they are first encoded into sequences of spikes which are used for training a PSNN model through unsupervised STDP. Before applying unsupervised learning, the SNN model needs to be initialised. In this experiment, we used the same mapped SNN model with a Talairach brain template and the same initial connections for all the individuals. Then, the connections were modified through the STDP learning with different sets of training samples for different individuals.

The trained model is later tested using the EEG samples of the individual x which was excluded from the training phase. For the classification experiment, we built 67 models of PSNN, each of which was trained by different nearest neighbouring EEG samples to each individual. For instance, the PSNN models of six randomly selected individuals (2 samples per class) are visualised in Fig. 7. In the graphs shown in Fig. 7, the amount of spike communication between clusters of neurons, centred by input variables, is captured as the thickness of lines. The thicker the line, the more interactions between variables were measured during STDP learning in the PSNN model. The trained PSNN models can be used for classification of testing EEG samples belonging to the three classes: C1 (healthy group H), C2 (treatment group M), and C3 (patient group P). The spatiotemporal connectivity in each of the trained PSNN model is supported by quantitative information. We computed the average of connection weights in each PSNN (from classes H, MMT, OP) and performed a t-test as reported in Table 1.

Table 1. Average connection weights of 67 PSNN models (denoted by PSNN (avg-CW), each was trained with different sets of nearest neighbouring samples to an individual from three classes: C1 (healthy group H), C2 (treatment group M), and C3 (patient group P). The p -value represents that the trained PSNN models of different groups of individuals were statistically significant with a high confidence, greater than 99%.

C1		C2		C3	
id	PSNN(avg-CW)	id	PSNN(avg-CW)	id	PSNN(avg-CW)
1	0.06	1	0.1	1	0.08
2	0.08	2	0.19	2	0.07
3	0.07	3	0.19	3	0.12
4	0.01	4	0.12	4	0.07
5	0.09	5	0.18	5	0.15
6	0.07	6	0.1	6	0.08
7	0.08	7	0.19	7	0.1
8	0.06	8	0.18	8	0.09
9	0.08	9	0.19	9	0.09
10	0.07	10	0.19	10	0.12
11	0.08	11	0.107	11	0.1
12	0.07	12	0.1	12	0.07
13	0.08	13	0.18	13	0.06
14	0.09	14	0.1	14	0.09
15	0.08	15	0.1	15	0.07
16	0.06	16	0.18	16	0.05
17	0.06	17	0.19	17	0.05
18	0.06	18	0.1		
19	0.06	19	0.1		
20	0.09	20	0.19		
21	0.08	21	0.17		
		22	0.19		
		23	0.18		
		24	0.18		
		25	0.17		
		26	0.19		
		27	0.19		
		28	0.19		
		29	0.15		

t-test results:
t-test(C1, C2)=1E-13<0.05
t-test(C1, C3)=0.04<0.05
t-test(C2, C3)=3E-09<0.05

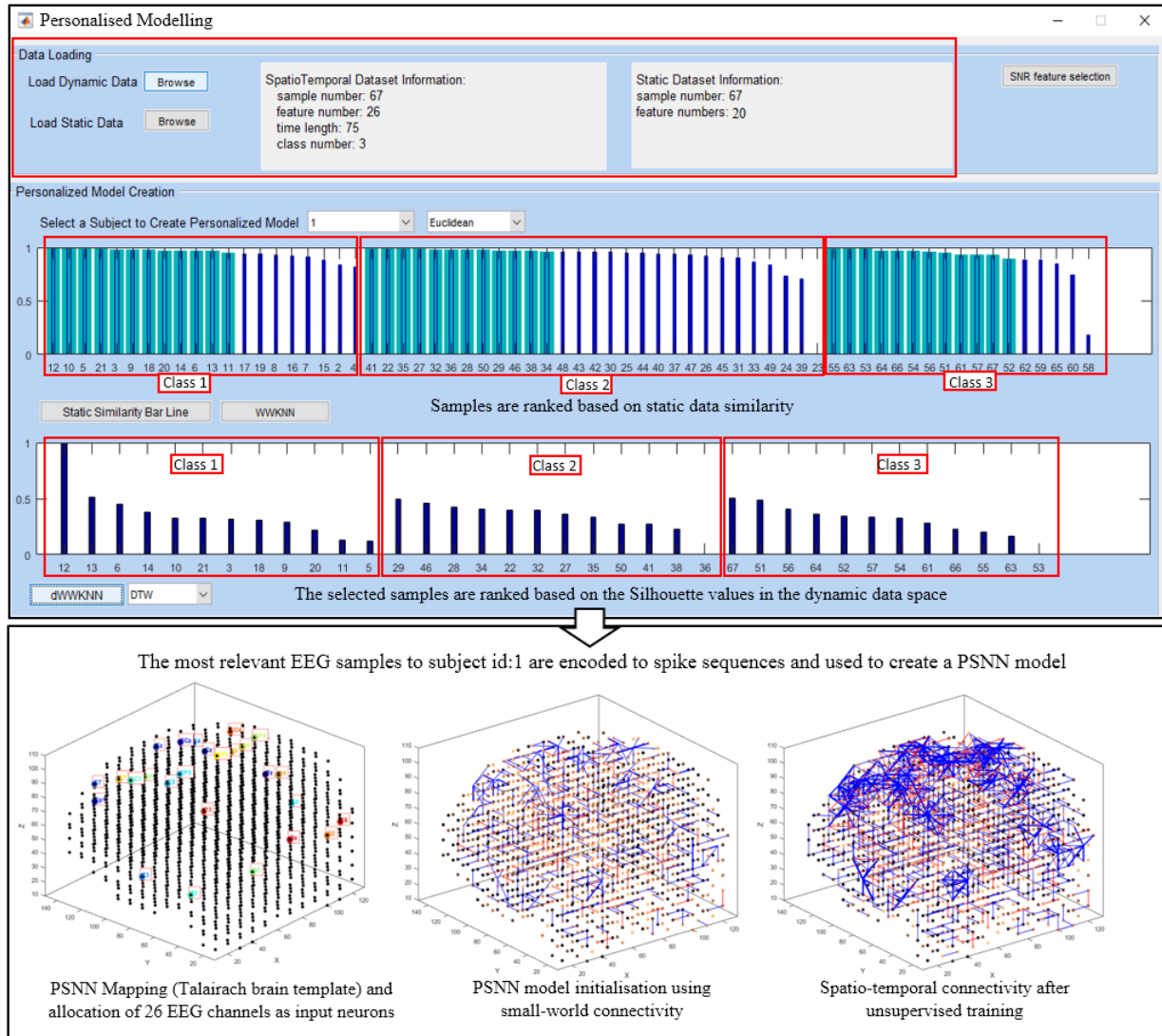


Fig. 6. The user interface of the in-house developed PSNN system, where the static and dynamic datasets are loaded (in this example the static clinical information and spatiotemporal EEG data of 67 individuals from class1: healthy subjects, class 2: patients undertaking treatments, and class 3: opiate addict patients). For an individual (e.g. subject id: 1), all samples in each class are ranked with respect to their similarity to id: 1. The top similar samples are highlighted in green (greater than a distance threshold α). The EEG data of the green coloured samples are selected, and then their pairwise DTW distances are computed in each class. The DTW distances are used to compute their Silhouette coefficient as new ranking measures for the samples. Samples with Silhouette value higher than a threshold s_θ and a high-density in neighbourhood are selected as the final cluster to train a PSNN model.

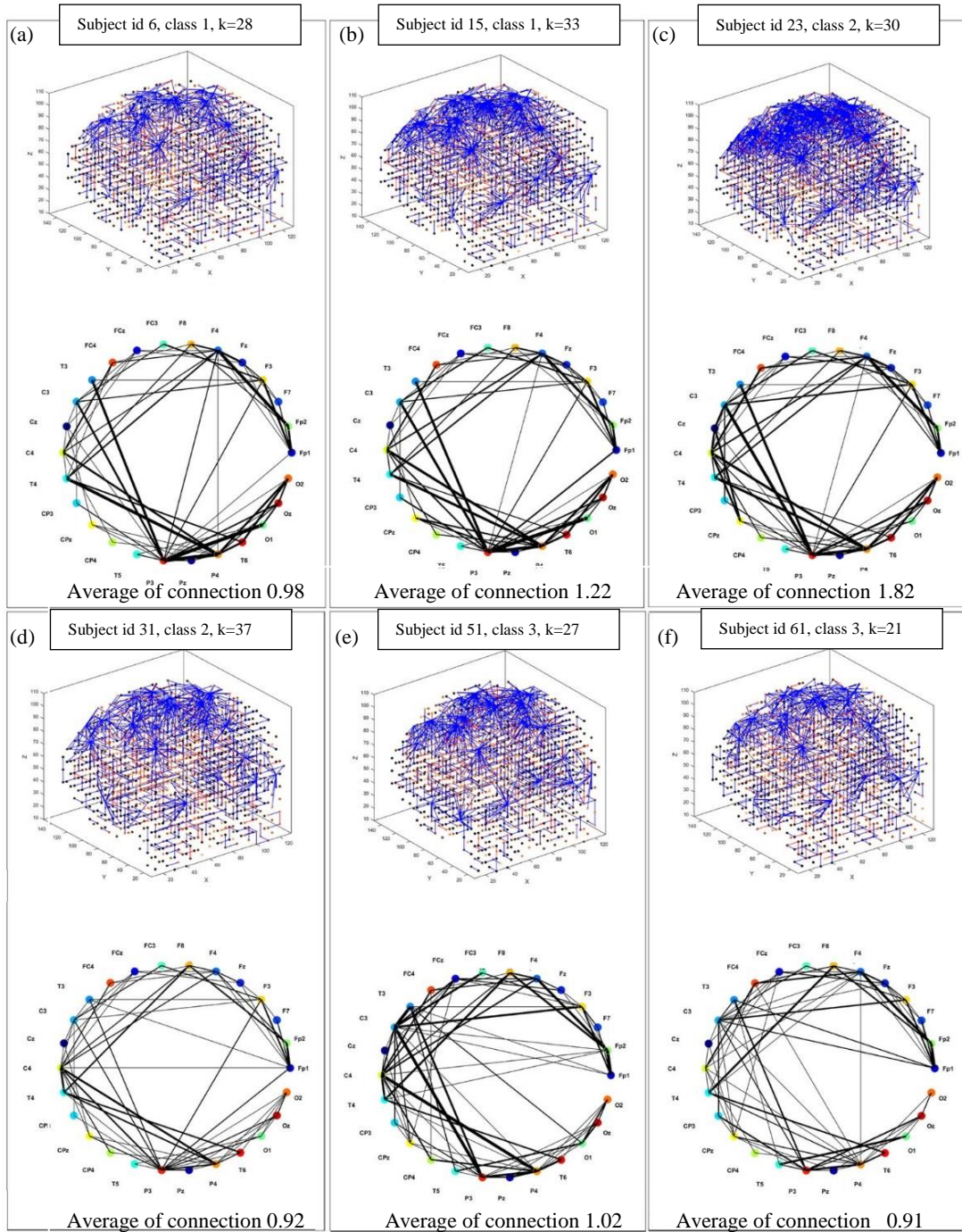


Fig. 7. PSNN models were created for six persons' data from class 1 (healthy control group in (a) and (b)), class 2 (Methadone treatment group in (c) and (d)), and class 3 (opiate addict group in (e) and (f)). Each PSNN model was trained on the temporal EEG data of the K nearest samples to the corresponding person using STDP unsupervised learning so that the spatiotemporal connectivity was adapted. Blue lines represent excitatory synapses (positive connections), whereas red lines refer to inhibitory synapses (negative connections). The spatiotemporal interactions between EEG channels are captured in a graph, where each node is a cluster of neurons around the corresponding EEG channel and each line between two clusters represents the amount of spike exchanged between these clusters.

The d2WKNN procedure was performed for all the 67 individuals to build 67 PSNN models for classification task and the overall accuracy of testing was reported in Table 2. The PSNN models were optimised using a grid-search method to achieve the best accuracy of classification. The optimised parameters were distance threshold α , Silhouette s_θ and the STDP learning rate α . The average parameters across all the 67 PSNN models are reported in Table 2.

Every PSNN model was trained using a different number of K nearest samples, selected with respect to the density of samples that are positioned inside the neighbourhood radius (thresholds α and s_θ). Therefore, In Table 2, we have reported the average K across all the PSNN models 67 individuals.

The PSNN was compared with a global SNN model in which all the individuals' data were used to build a model regardless of differences in individuals' personal information. The classification accuracy was also compared with traditional methods: Multiple Linear Regression (MLR), Support Vector Machine (SVM), Multi-Layer Perceptron (MLP) and Evolving Clustering Method (ECM) [51] as shown in Table 2. The SVM optimal parameters that resulted in the best classification accuracy were found after performing the experiments several times with different parameter setting (polynomial degree within [2, 5] and (RBF) kernel degree within [0.2, 1]). As shown in Table 2, when we used SVM for classification, the best accuracy was obtained using Kernel polynomial degree: 2. The MLP optimal parameters were also found after performing the experiments several times using different parameter settings (learning rate (LR) = [0.01, 0.5], momentum (M) = [0.1, 0.9], training iteration (TI) = [500, 1500], and number of hidden layer (HL) = [2, 6]).

In Table 3, the proposed d2WKNN clustering approach was replaced by different clustering methods (WWKNN [9], WKNN, and KNN) towards building PSNN models for classification. In all of these comparisons, the proposed PSNN models using W2WKNN method have achieved a higher classification accuracy of 83% with F-score=82%.

Table 2. Classification accuracy using the PSNN (based on d2WKNN) versus using a global SNN. C1 is a healthy control group, C2 is the treatment group and C3 is the patient group. Optimised parameters are distance threshold α , Silhouette threshold s_θ and the STDP learning rate α . The rest of the parameters were fixed as follows: spike-encoding threshold= 0.5; small-world connectivity radius= 2.5; neuron firing threshold= 0.5; LIF parameters (refractory time= 6 and potential leak rate=0.002); deSNN parameters (mod=0.4 and drift=0.25).

Personalised modelling of 67 trained PSNN models for each individual's data							
	Correctly classified	Accuracy in %	F-score	Parameters, averaged across all the 67 PSNN models	K nearest samples, averaged across all the 67 PSNN models		
C1	17 out of 21	81%	82%	$\alpha=0.67$	33.5		
C2	25 out of 29	86%		$s_\theta=0.74$			
C3	14 out of 17	82%		$\alpha=0.01$			
Overall accuracy		83%					
A global SNN of all individuals' data tested via leave-one-out cross-validation method							
	C1	C2	C3	Accuracy in %	F-score	$\alpha= -$	
C1	16	3	2	76%	67%	Leave-one-out cross-validation: training with 66 samples and tested with one holdout sample (repeated 67 times)	
C2	4	19	6	65%			
C3	2	6	11	65%			
Overall accuracy				68%		$s_\theta= -$	
						$\alpha=0.008$	
Classification accuracy using conventional methods							
Methods	SVM		MLR		MLP		ECM
Accuracy %	61%		60%		63%		63%
F-score	58%		60%		58%		61%
Optimised parameters	Kernel polynomial degree: 2		Learning-rate=0.01 Hidden layers = 4		Learning-rate=0.03 Momentum=0.4 Training-iteration=1000 Hidden layers = 4		Radius value=0.2

Table 3. Classification accuracy obtained using PSNN models with different clustering approaches (d2WKNN, WWKNN, WKNN, and KNN) for selecting the nearest neighbouring samples to an individual. Optimised parameters are distance threshold α , Silhouette threshold s_θ and the STDP learning rate α . The rest of the parameters were fixed as follows: spike-encoding threshold= 0.5; small-world connectivity radius= 2.5; neuron firing threshold= 0.5; LIF parameters (refractory time= 6 and potential leak rate=0.002); deSNN parameters (mod=0.4 and drift=0.25).

Method	Proposed d2WKNN	WWKNN [9]	WKNN	KNN
Accuracy	83%	75%	71%	69%
F-score	82%	75%	70%	65%
Parameters	$\alpha=0.67$ $s_\theta=0.74$ $\alpha=0.01$	$\alpha=0.61$ $s_\theta= -$ $\alpha=0.008$	$\alpha=0.6$ $s_\theta= -$ $\alpha=0.006$	$\alpha=0.67$ $s_\theta= -$ $\alpha=0.008$
K (on average)	33.5	49.4	48.9	48.5

Our findings show that the trained PSNN models (based on the integration of different data domains by d2WWKNN clustering approach) not only can distinguish samples with respect to their class labels with a higher classification accuracy, but also they can be used for a better understanding of interactions between spatiotemporal variables in each person's data (shown in the graphs in Fig. 7).

Fig. 7 illustrates that for one individual, one profile is created that assists an end-user (e.g., medical practitioner) with a personal interpretation of the interactions between features (in this case, different brain cortical areas measured by EEG). These personalised profiles support the model's interpretability and can explain what interactions between the cortical areas in the brain have led the PSNN model to categorise a person to a certain outcome (e.g. opiate addict). It can be seen from Fig 7(e) and (f) that although these two PSNN models belong to the same group of individuals (both from opiate addict group), their trained individualised models captured different relationships between the EEG variables. For example, Fig. 7(e) shows greater spike interactions between C3, T3 and P3 channels than other channels when compared with Fig. 7(f). This finding suggests great spatiotemporal interactions between the corresponding cortical areas (central, temporal and parietal areas) for this person in P group. On the other hand, the PSNN model of another opiate addict person, shown in Fig. 7(f), represents different levels of indications between these EEG channels. This personal interpretation represents that the PSNN models here are not acting as "black-box" information processing systems, but rather they are capable of revealing the personal "hidden" leaning patterns (adaptation of spatiotemporal connections) in the SNN models, which were not so far investigated in depth.

3.2 Case Study 2: Personalised Modelling for Prediction of an Individual's Risk of Stroke Occurrence in Relation to Environmental Conditions

At this section, the proposed personalised modelling system was applied to a case study of stroke data for early prediction of risk of stroke occurrence with respect to both static clinical information of patients and the temporal environmental data around them. Here, we present that the proposed PSNN models resulted in a higher accuracy of risk prediction when we integrated the static health data with some external risk factors (environmental changes).

The environmental data were recorded by Auckland Council from 12 variables positioned in Auckland over one year from 1st January 2002 to 31st December 2002. The environmental variables are: (1): wind-velocity

[knots], where Knots is a unit of velocity and is equivalent of 1.852 Kilometres per hour; (2): wind-direction average [Degrees]; (3): dry-bulb temperature [$^{\circ}\text{C}$]³; (4): wet-bulb temperature [$^{\circ}\text{C}$]; (5): barometric pressure [hPa]; (6): minimum-temperature; (7): maximum-temperature; (8): relative humidity [%], that is ratio of total moisture content of air to the maximum moisture the air can hold at a specific temperature; (9): solar irradiance [MJ/m^2]⁴; (10): Nitrogen Dioxide (NO_2) is a prominent air pollution that in presence of water can form nitric acid and nitrous acid; (11): Ozone (O_3) gas is an allotrope of oxygen that absorbs most of the UV radiation from the Sun; and (12): Sulphur dioxide (SO_2) is a toxic gas that is a by-product of combusting fossil fuels contaminated with sulphur. In presence of water and oxygen, sulphuric acid can be produced. This data was previously used in other publications [52], [9]. In total, 365 daily basis samples were recorded during this one year from all these 12 variables.

The static vector-based dataset of stroke consists of 1,207 individuals (all had stroke occurrence in the past) recorded from the 1st March 2002 to 31 December 2002. Each individual's sample is defined by four features: age, gender, stroke history, and current smoking statuses.

For every patient x in this dataset, a cluster of K nearest individuals to x is selected with respect to the distance measurement between static data of x to the rest of 1,206 individuals (after applying equations (2) and (3) from Section 2.1). Then, for every selected individual in this cluster, two periods of the environmental data are extracted, one corresponds to a 30-day interval before the stroke (called high-risk environmental sample) and the other one relates to a 30-day interval from one month before the stroke (called low-risk environmental sample). Therefore, for every individual, two temporal environmental samples are extracted. It means that for k selected individuals, there are $2k$ environmental samples, each represents the environmental changes over a 30-day period.

³ Celsius is the unit of temperature.

⁴ Megajoules per square meter is the amount of energy solar radiation received by one meter square during the day.

Fig. 8 shows an example of two-time intervals of environmental data that belong to “high-risk” versus “low-risk” temporal samples, categorised with respect to their time-distance from the onset of stroke for an individual who had stroke on 2nd June 2002. Afterwards, the environmental samples are subsampled again by computing the Silhouette coefficient with respect to the DTW distance as explained in Section 2.1, equations (5) and (6). The final selected environmental samples are then encoded into spikes and used for building a 3D PSNN model for this person. The model is trained using the whole spike trains of the training data and tested using a smaller length of the temporal samples of individual x (excluded from training) for early prediction of the likelihood of stroke occurrence.

Fig. 9 shows the in-house developed user interface of the proposed personalised predictive system, where 1,207 individuals’ static vector-based data are loaded along with 365 daily measurements of temporal environmental data. In this example, the person id: 361 is randomly selected, and a 3D PSNN model is created using the most relevant neighbouring samples to id: 361. The PSNN model spatially maps the highly correlated environmental variables to nearby input neurons. When the unsupervised STDP learning is performed, the spatiotemporal connectivity in the PSNN model is adapted with respect to input spike sequences of the environmental samples.

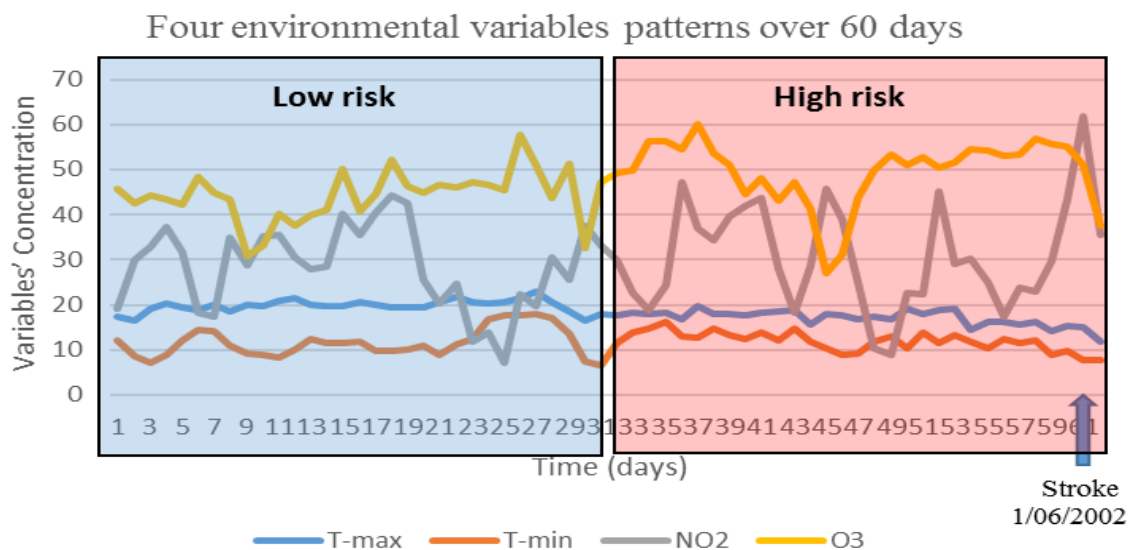


Fig. 8. An example of two temporal samples (belong to patient id: 361) of class high-risk and low-risk, each has a length of 30-day environmental measurement. For this patient, the interaction between temporal variables (e.g., O_3 , NO_2 , T-min, and T-max) will be learnt in a PSNN model to predict the risk of stroke earlier. Here, only four variables are visualised, but we used all the 12 variables in the prediction experiment.

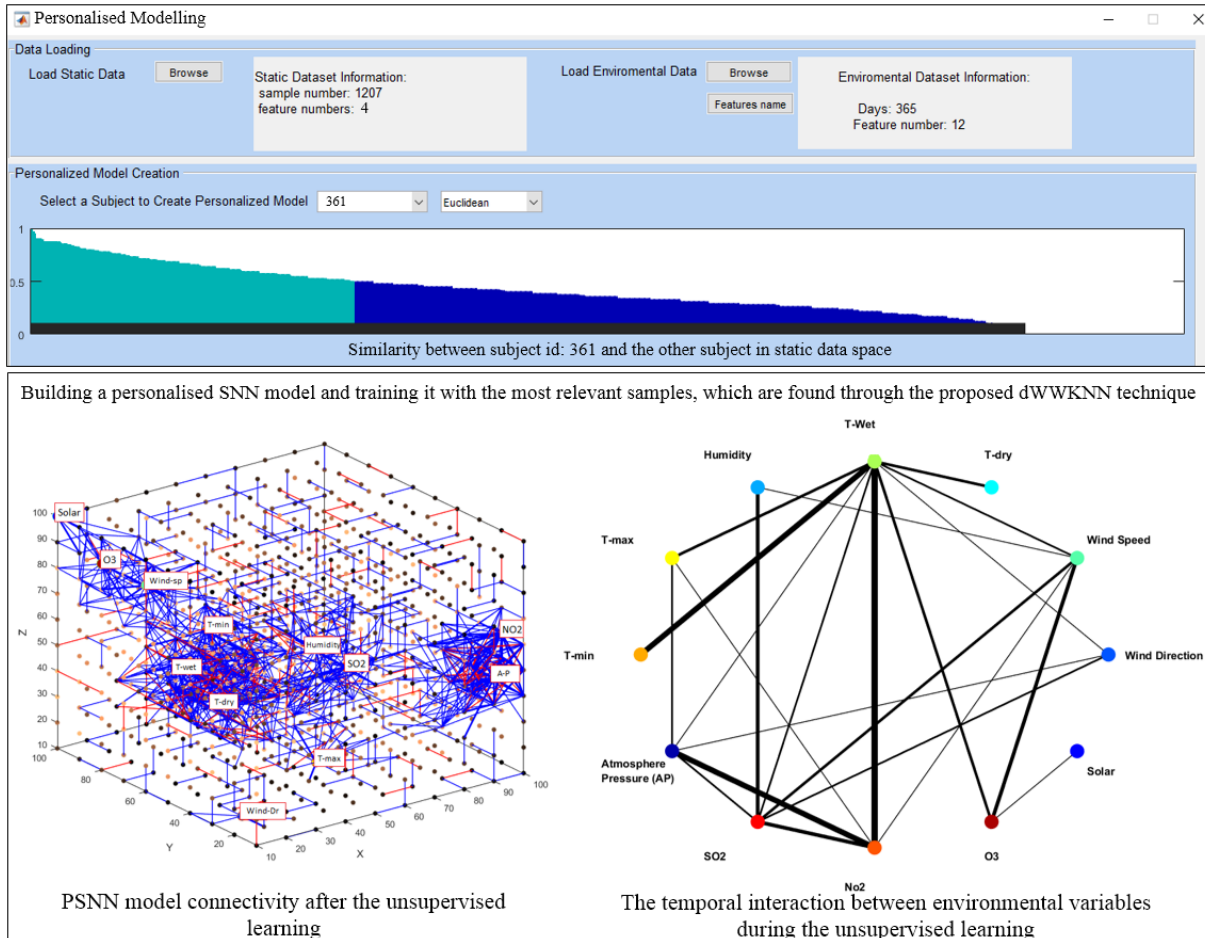


Fig. 9. The user interface of the proposed personalised predictive system for prediction of risk of stroke. A PSNN model is created to spatially map the environmental variables, where the most correlated variables are mapped to closer input neurons. Then the PSNN model was trained on the temporal spike sequences using STDP unsupervised learning to adapt the model connections. Blue lines represent excitatory synapses (positive connections), whereas red lines refer to inhibitory synapses (negative connections). In the graph, the amount of spike communication between clusters of neurons, centred by input variables, is captured as the thickness of lines. The thicker the line, the more interactions between variables during STDP learning.

The temporal interaction between environmental variables is shown in a graph, where the vertexes represent the variables and arcs are weighed by the amount of the spike communications between the variables during the learning process.

Fig. 10(a) illustrates the accuracy of personalised prediction of risk of stroke for patient id: 361, where the high-risk and low-risk environmental samples were perfectly predicted around 10 days pre-stroke. It can be seen here that the trained PSNN model was tested by different lengths of the testing samples to identify the earlier time point for the best possible prediction. It means that for every person, one PSNN model was

created and trained, then it was tested 26 times with testing samples of different lengths (30 days, 29 days, and stepdown to 5 days of environmental data). This procedure was repeated 45 times in a grid-search optimisation algorithm with different combinations of parameters α , s_θ and ∞ as shown in relation (13).

The personalised models were created for all 1,207 individuals. Then we selected a subset of individuals who their testing samples were correctly predicted in at least 15 out of 26 validation rounds. We found that personalised modelling was successfully performed for 655 patients, suggesting that the external environmental data were considered as external risk factors to increase the risk of stroke for this subset of population. Fig. 10(b) illustrates a high average accuracy of prediction (from 80% to 93%) around 15 days pre-stroke for only these 655 individuals. For the rest of the individuals, the PSNN models did not capture any meaningful relationships between the temporal environmental changes and the static health information that could increase the risk of stroke. This new finding sounds rational as the environmental changes are not the only risk factors to trigger a stroke occurrence, but they were discovered here as additional influential factors that affected only a subset of individuals who were sensitive to environmental circumstances.

In Table 4, the proposed d2WKNN clustering approach was replaced by different clustering methods (WKNN, WKNN, and KNN) for building PSNN models. The PSNN models using W2WKNN method have achieved a higher prediction accuracy of 86.5% which is the average of the accuracy in 15 days before stroke (80%) and the accuracy of one day before stroke (93%) with F-score=80%. The optimised parameters were distance threshold α and Silhouette threshold s_θ in the d2WKNN method and the STDP learning rate ∞ as reported in Table 4.

In addition to achieving a higher accuracy when compared with conventional methods, our findings suggest that personalised modelling based on the integration of static health data and temporal environmental data was promising to discover the hidden association patterns between these two data domains and risk factors.

It can be seen from Fig. 9 that the personalised profile of an individual (in this example patient id: 361) enhanced the model interpretability and allowed to understand what changes in the environmental data have led to increasing the risk of stroke for this patient. For instance, Fig. 9 illustrates that NO_2 and wet-bulb temperature variables have shown great interactions with other variables during the 7-day period prior to stroke, meaning that they have highly influenced many of the other environmental variables to change over time. The relationships between environmental variables are complex as any variable can influence the other ones, either directly or indirectly. Here, the proposed personalised modelling created an interpretable model of environmental interactions that contributed to detecting the effects of external factors that potentially increased the risk of stroke for an individual (in this example for id: 361).

From thermodynamics perspective, the detected interaction between the variables in the trained PSNN model is expressive as it shows the effects of NO_2 and SO_2 on the temperature (wet and dry bulb temperatures) during the 7-day period. This can be explained by the fact that these gases are categorised as indirect greenhouse gases [53]. This means, although NO_2 and SO_2 are not directly affecting the local temperature, they would react with other gases to form direct greenhouse gases that are contributing in temperature variation [53], [54], [55], [56]. These interactions were clearly captured during the learning process in the PSNN model with 7-day environmental data prior to stroke, as shown in Fig. 9.

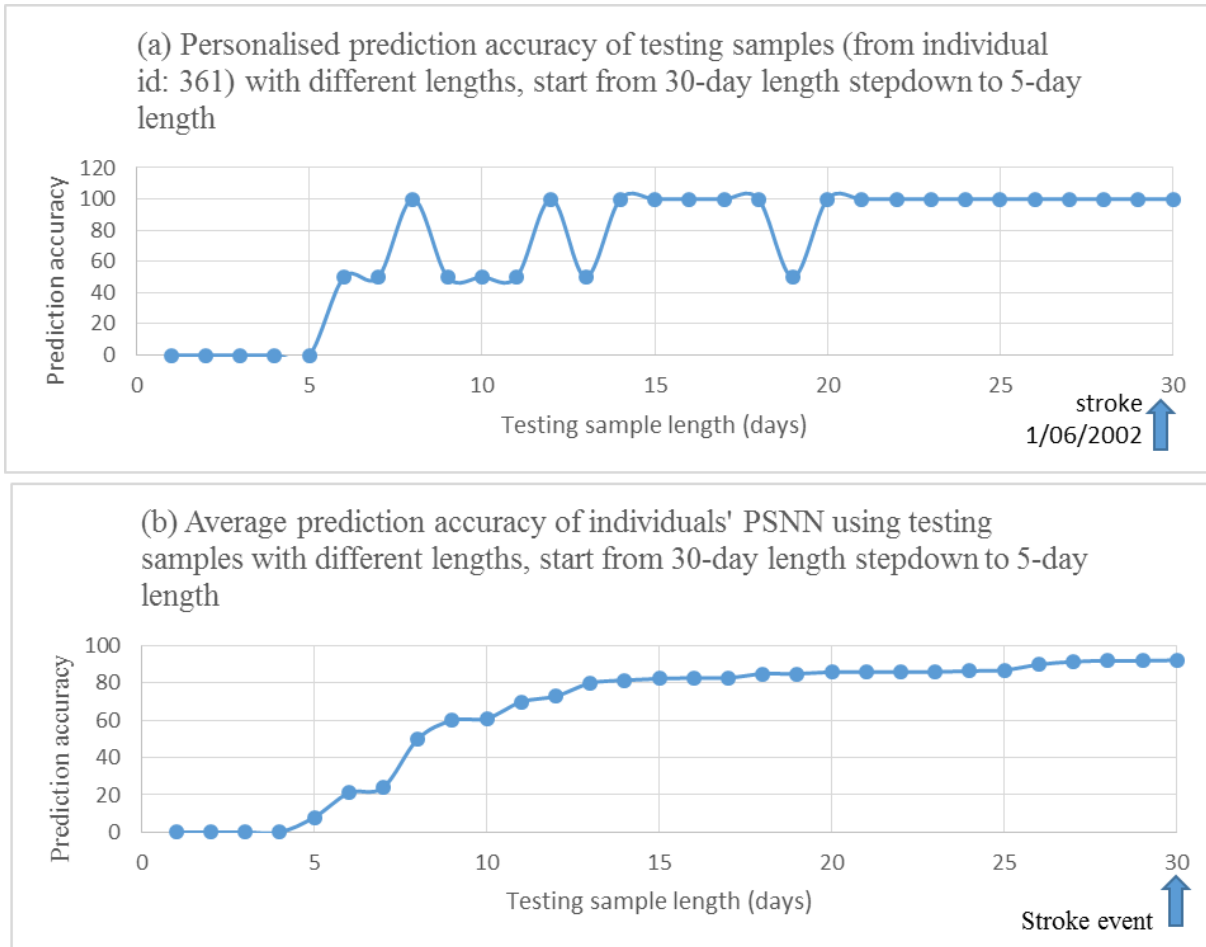


Fig. 10. (a) Example of personalised prediction of risk of stroke occurrence for one randomly selected person (id: 361). The PSNN is trained on the whole length of training samples and tested on different lengths of the testing samples; (b) the average prediction accuracy of 655 individuals' PSNN models. It shows that the longer past data is used, the more accurate the individual prediction is, with a small improvement after 14 days.

Table 4. Comparative analysis of the average prediction accuracy obtained using PSNN models with different clustering approaches (d2WKNN, WWKNN [9], WKNN and KNN) for selecting the nearest neighbouring samples to an individual. The accuracy is an average of the accuracy in 15 days before stroke and the accuracy of one day before stroke. Optimised parameters are distance threshold α , Silhouette threshold s_θ and the STDP learning rate α . The rest of the parameters were fixed as follows: spike-encoding threshold= 0.5; small-world connectivity radius= 2.5; neuron firing threshold= 0.5; LIF parameters (refractory time= 6 and potential leak rate=0.002); deSNN parameters (mod=0.4 and drift=0.25).

Method	Proposed	d2WKNN	WWKNN [9]	WKNN	KNN
Accuracy	86.50		78.00	73.00	70.00
F-score	85.00		75.00	70.00	70.00
Optimised parameters	$\alpha=0.73$ $s_\theta=0.54$ $\alpha=0.006$		$\alpha=0.77$ $s_\theta=-$ $\alpha=0.001$	$\alpha=0.69$ $s_\theta=-$ $\alpha=0.01$	$\alpha=0.75$ $s_\theta=-$ $\alpha=0.01$
K (on average)	378.4		459.6	558.4	573.9

4. Discussions and Future Directions

The feasibility analysis of the proposed approach was validated here using two different case studies, but further studies are required to determine generalisability to other populations with different types of data and a greater number of samples. The future implementation pathway is e-Health application development in medical practice for the prediction of risk factors along with the detection of causal and temporal interactions between factors, expressed as data variables. In this direction, we aim to develop methods for extracting deep spatiotemporal knowledge from trained personalised models that can be used for a personalised health risk profiling and a better understanding of personal and group health factors [57].

Also, it should be mentioned that the optimisation method used in this paper was a grid-search on combination of parameters. Each parameter was searched within a specified range. In this paper, the parameters of d2WKNN (s_θ and α) as well as the STDP learning rate parameter α were optimised. The rest of the parameters in SNN were fixed with respect to previous experiments as follows: spike-encoding threshold= 0.5; small-world connectivity radius= 2.5; neuron firing threshold= 0.5; LIF parameters (refractory time= 6 and potential leak rate=0.002); deSNN parameters (mod=0.4 and drift=0.25). To improve the system's performance, the optimisation procedure needs to be further improved to consider all the possible ranges of the SNN parameters and the d2WKNN method.

5. Conclusion

This research introduced a novel personalised modelling system based on a new clustering approach, named d2WKNN, which extracts a subset of nearest neighbouring samples to an individual with respect to the integration of static (vector-based) and temporal/spatiotemporal data domains. The learning process in the proposed personalised modelling is performed in an SNN architecture, which captures both *spatial* and *temporal* information in a unifying model.

The system was applied to two case studies: (1) classification of spatiotemporal neuroimaging data for the investigation of response to treatment and (2) prediction of risk of stroke with respect to temporal environmental data.

The personalised SNN models based on the d2WKNN method have improved the accuracy and the interpretability of the models. The system also supported personalised profiling for every person's data that allowed for a better understanding of the relationships between the model's features and the predicted outcomes.

The proposed PSNN model based on d2WKNN resulted in a higher prediction/classification accuracy of 80% to 93% with F-score=80% when compared to the models generated based on WWKNN [9], WKNN, and KNN clustering methods. It also performed superior when compared with conventional classification methods, such as SVM and MLP. The hyper-parameters of the proposed system, including the PSNN models and the clustering parameters, were optimised for each individual.

This personalised modelling system can facilitate knowledge discovery by capturing patterns of spatiotemporal/temporal interactions between the variables in a 3-dimensional personalised SNN architecture by extracting deep spatiotemporal rules. Therefore, unlike the conventional machine learning and statistical analysis methods, which receive input data, process them and produce outputs, performing like a "black-box", the PSNN system supports the outcome prediction/classification results with an interpretation of the interactions between features in the model. It can be used as a decision support system to help specialists (e.g. medical practitioner) to justify certain medical decisions for an individual.

Acknowledgment

This research is supported by Knowledge Engineering and Discovery Research Institute (<https://kedri.aut.ac.nz/>), AUT. The authors would like to acknowledge Dr Grace Wang from AUT, Dr Bruce Russell and Professor Robert Kydd from the University of Auckland for providing us with the EEG

data which the ethical approval was granted by the “Northern X Regional Ethics Committee of New Zealand”. The stroke-related data was first published and collected by Prof Valery Feigin and his group in National Institute for Stroke and Applied Neurosciences (<http://www.aut.ac.nz/research/professors-at-aut/valery-feigin>), Auckland University of Technology, New Zealand. We also acknowledge Barry Dowdeswell for proofreading the paper.

References

- [1] Y.-F. Lu, D. Goldstein, M. Angrist and G. Cavalleri, “Personalized medicine and human genetic diversity,” *Cold Spring Harbor perspectives in medicine*, p. a008581, 2014.
- [2] W.-S. Chu, F. De la Torre and J. F. Cohn, “Selective Transfer Machine for Personalized Facial Expression Analysis,” *IEEE transactions on pattern analysis and machine intelligence*, vol. 39, no. 3, pp. 529-545, 2017.
- [3] N. Kasabov, “Global, local and personalised modeling and pattern discovery in bioinformatics: An integrated approach,” *Pattern Recognition Letters*, vol. 28, no. 6, pp. 673-685, 2007.
- [4] N. Kasabov, “NeuCube: A spiking neural network architecture for mapping, learning and understanding of spatio-temporal brain data,” *Neural Networks*, vol. 52, pp. 62-76, 2014.
- [5] A. Racine, M. Rickhouse, D. Wolk and B. Dickerson, “The personalized Alzheimer's disease cortical thickness index predicts likely pathology and clinical progression in mild cognitive impairment,” *Alzheimer's & Dementia: Diagnosis, Assessment & Disease Monitoring*, vol. 10, pp. 301-310, 2018.
- [6] T. J.-P. Njafa and N. S. Engo, “Quantum associative memory with linear and non-linear algorithms for the diagnosis of some tropical diseases,” *Neural Networks*, vol. 97, pp. 1-10, 2018.
- [7] H. Gao, A. Aderhold, K. Mangion, X. Luo, D. Husmeier and C. Berry, “Changes and classification in myocardial contractile function in the left ventricle following acute myocardial infarction,” *Journal of The Royal Society Interface*, vol. 14, no. 132, p. 20170203, 2017.
- [8] K. Mangion, H. Gao, D. Husmeier, X. Luo and C. Berry, “Advances in computational modelling for personalised medicine after myocardial infarction,” *Heart*, vol. 104, no. 7, pp. 550-557, 2018.
- [9] N. Kasabov, V. Feigin, Z. Hou, Y. Chen, L. Liang, R. Krishnamurthi, M. Othman and P. Parma, “Evolving spiking neural networks for personalised modelling, classification and prediction of spatio-temporal patterns with a case study on stroke,” *Neurocomputing*, vol. 134, pp. 269-279, 2014.
- [10] N. Kasabov, M. G. Doborjeh and Z. Gholami, “Mapping, learning, visualization, classification, and understanding of fMRI Data in the NeuCube evolving spatiotemporal data machine of spiking neural networks,” *IEEE transactions on neural networks and learning systems*, vol. 28, no. 4, pp. 887-899, 2017.
- [11] M. G. Doborjeh, N. Kasabov and Z. Gholami, “Evolving, dynamic clustering of spatio/spectro-temporal data in 3D spiking neural network models and a case study on EEG data,” *Evolving Systems*, pp. 1-17, 2017.
- [12] N. Kasabov and E. Capecci, “Spiking neural network methodology for modelling, classification and understanding of EEG spatio-temporal data measuring cognitive processes,” *Information Sciences*, vol. 294, pp. 65-575, 2015.

- [13] S. Dora, S. Suresh and N. Sundararajan, "Online Meta-neuron Based Learning Algorithm For A Spiking Neural Classifier}," *Information Sciences*, vol. 414, pp. 19-32, 2017.
- [14] G. Orchard, C. Meyer and R. Etienne-Cummings, "HFirst: A Temporal Approach to Object Recognition," *IEEE transactions on pattern analysis and machine intelligence*, vol. 37, no. 10, pp. 2028-2040, 2015.
- [15] F. Faghihi and A. A. Moustafa, "Sparse and burst spiking in artificial neural networks inspired by synaptic retrograde signaling," *Information Sciences*, vol. 421, pp. 30-42, 2017.
- [16] N. Kasabov, *Evolving Connectionist Systems: The Knowledge Engineering Approach*, Springer, 2007.
- [17] D. J. Berndt and J. Clifford, "Using dynamic time warping to find patterns in time series," in *KDD workshop*, vol. 10, 1994, pp. 359-370.
- [18] P. J. Rousseeuw, "Silhouettes: a Graphical Aid to the Interpretation and Validation of Cluster Analysis," *Computational and Applied Mathematics*, pp. 53-65.
- [19] E. M. Izhikevich, "Polychronization: Computation with Spikes," *Neural Computation*, vol. 18, no. 2, pp. 245-282, 2006.
- [20] R. Brette, M. Rudolph, T. Carnevale, M. Hines, D. Beeman, J. M. Bower, M. Diesmann, A. Morrison, P. H. Goodman, J. Harris and C. Frederick, "Simulation of Networks of Spiking Neurons: A Review of Tools and Strategies," *Journal of Computational Neuroscience*, vol. 23, no. 3, pp. 349-398, 2007.
- [21] W. Maass, "Networks of Spiking Neurons: the Third Generation of Neural Network Models," *Neural Networks*, vol. 10, no. 9, pp. 1659-1671, 1997.
- [22] C. W. Anderson, E. A. Stolz and S. Shamsunder, "Multivariate autoregressive models for classification of spontaneous electroencephalographic signals during mental tasks," *IEEE Transactions on Biomedical Engineering*, vol. 45, no. 3, pp. 277-286, 1998.
- [23] W. Maass, N. Thomas and M. Henry, "Real-time computing without stable states: a new framework for neural computation based on perturbations," *Neural Computation*, vol. 14, no. 11, p. 2531-2560, 2002.
- [24] T. Delbruck, "jaer open source project," 2007. [Online]. Available: <https://sourceforge.net/p/jaer/wiki/Home/>. [Accessed 15 10 2014].
- [25] N. Kasabov, L. Zhou, M. G. Doborjeh, Z. Gholami and J. Yang, "New Algorithms for Encoding, Learning and Classification of fMRI Data in a Spiking Neural Network Architecture: A Case on Modelling and Understanding of Dynamic Cognitive Processes," *IEEE Transactions on Cognitive and Developmental Systems*, 2016.
- [26] K. Dhoble, N. Nuntalid, G. Indiveri and N. Kasabov, "Online spatio-temporal pattern recognition with evolving spiking neural networks utilising address event representation, rank order, and temporal spike learning," in *IEEE World Congress on Computational Intelligence*, Brisbane, Australia, 2012.
- [27] N. Sengupta and N. Kasabov, "Spike-time encoding as a data compression technique for pattern recognition of temporal data," *Information Sciences*, vol. 406, p. 133-145, 2017.
- [28] B. Schrauwen and J. Van Campenhout, "BSA, a fast and accurate spike train encoding scheme," in *Proceedings of the international joint conference on neural networks*, 2003.
- [29] S. M. Bohte, "The evidence for neural information processing with precise spike-times: A survey," *Natural Computing*, vol. 3, no. 2, pp. 195-206, 2004.
- [30] P. h. Pearson, *biological science*, 2 ed., 2005.
- [31] B. W. Knight, "Dynamics of encoding in a population of neurons," *The Journal of general physiology*, vol. 59, no. 6, pp. 734-766, 1972.
- [32] J. Talairach and P. Tournoux, "Co-planar stereotaxic atlas of the human brain. 3-Dimensional proportional system: an approach to cerebral imaging," in *Thieme Medical Publishers.*, New York, 1988.

- [33] E. Tu, N. Kasabov and J. Yang, "Mapping Temporal Variables Into the NeuCube for Improved Pattern Recognition, Predictive Modeling, and Understanding of Stream Data," *IEEE Transactions on Neural Networks and Learning Systems*, vol. 28, no. 6, pp. 1305-1317, 2017.
- [34] D. Verstraeten, B. Schrauwen, M. D'Haene and D. Stroobandt, "An experimental unification of reservoir computing methods," *Neural Networks*, vol. 20, no. 3, pp. 391-403, 2007.
- [35] J. Hu, Z.-G. Hou, Y.-X. Chen, N. Kasabov and N. Scott, "EEG-based classification of upper-limb ADL using SNN for active robotic rehabilitation," in *IEEE RAS/EMBS international conference on biomedical robotics and biomechatronics*, 2014.
- [36] E. Tu, N. Kasabov, M. Othman, Y. Li, S. Worner, J. Yang and Z. Jia, "NeuCube(ST) for Spatio-Temporal Data Predictive Modelling with a Case Study on Ecological Data," in *Neural Networks (IJCNN)*, Beijing, China, 2014.
- [37] E. Bullmore and O. Sporns, "Complex brain networks: graph theoretical analysis of structural and functional systems," *Nature Reviews Neuroscience*, vol. 10, no. 3, pp. 186-198, 2009.
- [38] V. Braitenberg and A. Schuz, *Cortex: statistics and geometry of neuronal connectivity*, Springer Berlin, 1998.
- [39] L. Lapique, "Recherches quantitatives sur l'excitation électrique des nerfs traitée comme une polarisation," *J. Physiol. Pathol. Gen.*, vol. 9, no. 1, pp. 620-635, 1907.
- [40] L. F. Abbott, "Lapicque's introduction of the integrate-and-fire model neuron (1907)," *Brain research bulletin*, vol. 50, no. 5, pp. 303-304, 1999.
- [41] E. M. Izhikevich, "Simple Model of Spiking Neurons," *IEEE Transactions on neural networks*, vol. 14, no. 6, pp. 1569-1572, 2003.
- [42] S. Song, K. D. Miller and L. F. Abbott, "Competitive Hebbian learning through spike-timing-dependent synaptic plasticity," *Nature neuroscience*, vol. 3, no. 9, pp. 919-926, 2000.
- [43] D. O. Hebb, *The Organization of Behavior: A Neuropsychological Approach*, John Wiley & Sons, 1949.
- [44] Y. LeCun, Y. Bengio and G. Hinton, "Deep learning," *Nature*, pp. 436-444, 2015.
- [45] J. Schmidhuber, "Deep Learning in Neural Networks: An Overview," *Neural Networks*, vol. 61, pp. 85-117, 2015.
- [46] N. Kasabov, K. Dhoble, N. Nuntalid and G. Indiveri, "Dynamic evolving spiking neural networks for on-line spatio-and spectro-temporal pattern recognition," *Neural Networks*, vol. 41, pp. 188-201, 2013.
- [47] S. Thorpe and J. Gautrais, "Rank order coding," in *Computational Neuroscience*, Springer, 1998, pp. 113-118.
- [48] M. Dobarjeh and N. Kasabov, "Personalised modelling on integrated clinical and EEG spatio-temporal brain data in the NeuCube spiking neural network system," in *International Joint Conference on Neural Networks (IJCNN)*, Vancouver, 2016.
- [49] G. Wang, R. Kydd, T. Wouldes, M. Jensen and B. Russell, "Changes in resting EEG following methadone treatment in opiate addicts," *Clinical Neurophysiology*, vol. 126, no. 5, pp. 943-950, 2015.
- [50] G. Wang, R. Kydd and B. Russell, "Auditory event-related potentials in methadone substituted opiate users," *Psychopharmacology*, vol. 29, no. 9, pp. 983-995, 2015.
- [51] Q. Song and N. Kasabov, "ECM — A Novel On-line, Evolving Clustering Method and Its Applications," *Foundations of Cognitive Science*, pp. 631-682, 2001.
- [52] V. Feigin, K. Carter, M. Hackett, P. Barber, H. McNaughton and L. Dyal, "Ethnic disparities in incidence of stroke subtypes: Auckland regional community stroke study, 2002–2003," vol. 5, no. 2, pp. 130-139, 2006.
- [53] K. Smith, M. Jerrett, R. H. Anderson, R. Burnett, V. tone, R. Derwent, R. tkinson, A. Cohen, S. Shonkoff and D. Krewski, "Public health benefits of strategies to reduce greenhouse-gas

- emissions: health implications of short-lived greenhouse pollutants," *The Lancet*, vol. 374, no. 9707, pp. 2091-2103, 2009.
- [54] J. Lelieveld and F. Dentener, "What controls tropospheric ozone?," *Journal of Geophysical Research: Atmospheres*, vol. 105, no. D3, pp. 3531-3551, 2000.
- [55] P. J. Crutzen, "The influence of nitrogen oxides on the atmospheric ozone content," *Quarterly Journal of the Royal Meteorological Society*, vol. 96, no. 408, pp. 320-325, 1970.
- [56] P. J. Crutzen, "Ozone production rates in an oxygen-hydrogen-nitrogen oxide atmosphere," *Journal of Geophysical Research*, vol. 76, no. 30, pp. 7311-7327, 1971.
- [57] N. Kasabov, *Time-Space, Spiking Neural Networks and Brain-Inspired Artificial Intelligence*, vol. 7, Springer, 2018.
- [58] J. A. Pe' rez-Carrasco, B. Zhao, C. Serrano, B. Acha, T. Serrano-Gotarredona, S. Chen and B. Linares-Barranco, "Mapping from Frame-Driven to Frame-Free Event-Driven Vision Systems by Low-Rate Rate Coding and Coincidence Processing-Application to Feedforward ConvNets," *IEEE transactions on pattern analysis and machine intelligence*, vol. 35, no. 11, pp. 2706-2719, 2013.